Electrophoretic Control of Reconstituted Adenine Nucleotide Translocation†

Reinhard Krämer* and Martin Klingenberg

ABSTRACT: The initial velocity of adenine nucleotide exchange catalyzed by the reconstituted ADP–ATP carrier from beef heart mitochondria was measured under the influence of membrane potential and with different nucleotide distributions between the internal liposomal and the external buffer volume. Both V_{max} and K_m of adenine nucleotide uptake not only changed due to the applied potential but also depended on the respective nucleotide distribution. The rate equations for the ADP–ATP exchange under the various conditions were derived. These equations were simplified by assuming two alternative situations: either (a) an affinity type model, where the membrane potential influences only the affinity of the adenine nucleotide carrier toward ATP and ADP, or (b) a velocity type or distribution model, where the membrane potential modulates the rate constants of the ADP–ATP exchange. On the basis of several simplifications in the reconstituted system, the rate equations could be solved and the rate constants and dissociation constants of the exchange in the "energized" and in the "deenergized" state could be calculated. These values were used to derive prediction tables for normalized exchange rates under different nucleotide distributions, which were then compared with the experimental data. Only the exchange rates predicted by the velocity-type model agreed with the measured values. On the basis of this model a definite asymmetry caused by the membrane potential could be seen. Whereas this asymmetry is not very pronounced in the case of carrier–ADP complexes, about 40 times more ATP-loaded binding sites face the outside than the inside of the vesicles in the energized state.

When mitochondria are energized by coupled electron transport, ADP and ATP are exchanged at different rates and differently in efflux and influx (Klingenberg & Pfaff, 1966; Klingenberg, 1975). The uptake of ATP is strongly suppressed in favor of that of ADP, and the efflux of ATP is increased compared to that of ADP. Although the membrane potential is known to be the primary energy source for the secondary active transport of ADP and ATP across the inner mitochondrial membrane (Klingenberg et al., 1969; LaNoue et al., 1978; Klingenberg & Rottenberg, 1977; Krämer & Klingenberg, 1980a), there are still questions about the mechanism of energy transduction and also controversial experimental data concerning this point.

The regulatory influence of the membrane potential on the ADP–ATP carrier activity can theoretically be explained by two different models. In the first, the affinity-type model, only the dissociation constants of the carrier–nucleotide complexes are changed by the membrane potential. As a result, under steady-state conditions the substrate is concentrated on the side with the higher dissociation constant. This mechanism, necessarily involving an energy-dependent conformational change of the carrier protein, is favored by two groups (Souverijn et al., 1973; Vignais et al., 1975; Villiers et al., 1979; Lauquin et al., 1978). In the second, the velocity-type model, the rate constants in both transport directions are different. Thus, the substrate binding sites are enriched on one side of the membrane. This model has also been called the distribution model. A regulation based on influences on the translocation rates has been postulated by us since the first findings that the adenine nucleotide exchange in mitochondria is energy dependent. An explicit differentiation between the change of affinity or rate was first pursued by analyzing the effect of energy on the competition between ADP and ATP (Klingenberg, 1972, 1980).

Also, in several other transport systems, experiments concerning the mechanism of carrier regulation based on the kinetic properties of the transport process have been carried out, e.g., aspartate–glutamate exchange in mitochondria (LaNoue et al., 1979; Murphy et al., 1979), lactose in *Escherichia coli* (Kaczorowski et al., 1979; Wright et al., 1979; Lancaster et al., 1975; Booth & Hamilton, 1980), hexose transport in *Chlorella* (Komor et al., 1973; Schwab & Komor, 1978), and sugar transport in erythrocytes (Geck, 1971; Holman, 1980).

This work is the first to obtain detailed kinetic information about a carrier mechanism with a reconstituted system. This system offers great advantages, since defined nucleotide distributions on both sides of the membrane can be established which proved to be essential for the kinetic resolution of the transport regulation. Under these provisions, the experimental data clearly demonstrate that the ADP–ATP exchange in mitochondria is regulated by the membrane potential, according to a velocity-type model.

Materials and Methods

Materials. The chemicals used and their sources were as follows: Triton X-100 (Sigma), egg yolk phospholipids (Merck), carboxyatractylate, valinomycin and nucleotides (Boehringer-Mannheim), radioactive nucleotides (NEM), Dowex 1-X8 (Bio-Rad), and Sephadex (Pharmacia). All other chemicals were of analytical grade. Hydroxylapatite was prepared as previously described (Krämer & Klingenberg, 1979).

Determinations. Protein concentration was determined by the method of Lowry in the presence of 1% sodium lauryl sulfate (Helenius & Simons, 1972), and phosphorus was estimated by the method of Chen et al. (1956).

Isolation of the Adenine Nucleotide Carrier. The carrier protein was isolated by hydroxylapatite chromatography in a batch procedure with Triton X-100 as described by Krämer & Klingenberg (1979).

Reconstitution of Adenine Nucleotide Exchange. Liposomes were prepared by sonication of phospholipids with a

† From the Institut für Physiologische Chemie, Physikalische Biochemie, und Zellbiologie der Universität München, 8000 München 2, Federal Republic of Germany. *Received May 18, 1981.* This work was supported in part by the Deutsche Forschungsgemeinschaft.

0006-2960/82/0421-1082$01.25/0

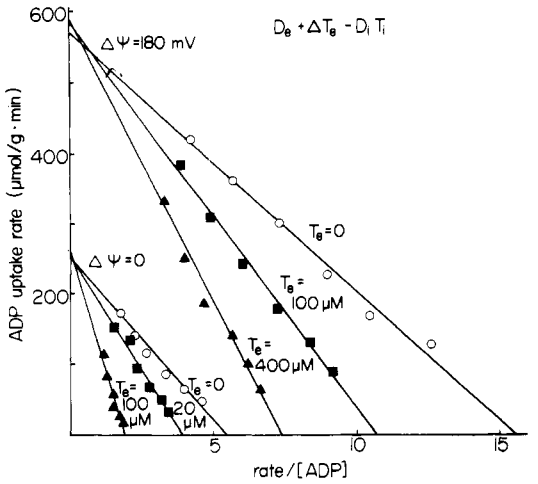

FIGURE 1: Competition of ADP and ATP uptake. Labeled external ADP was varied between 10 and 100 μM; addition of unlabeled external ATP is indicated in the figure. Internal ADP and ATP were 5 mM each. Every point includes an initial velocity determination as described under Materials and Methods.

Branson sonifier (Krämer et al., 1977). The carrier protein was incorporated (Krämer & Klingenberg, 1977a) and the ADP–ATP translocation activity was reconstituted by a freeze–thaw procedure (Kasahara & Hinkle, 1977) and a second sonication (Krämer & Klingenberg, 1979, 1977b). The sonication buffer was 200 mM NaCl or KCl, depending on the intended membrane potential, 10 mM Tricine–NaOH,[1] pH 8.0, and 10 mM nucleotides. The type of nucleotides is indicated in the corresponding experiment. The internal and external nucleotide distribution remains stable during the reconstitution procedure, since interfering activities of ATPase and adenylate kinase were virtually absent in the purified adenine nucleotide carrier preparation (Krämer & Klingenberg, 1980a). The membrane potential was adjusted as described by Krämer & Klingenberg (1980a). As it was already discussed in detail in the same paper, we emphasize that the value given for the membrane potential can only be calculated as Nernst potential and is certainly overestimated. Nevertheless, the potential is effectively influencing the direction of ATP–ADP exchange for longer than 10 min as it was also shown there. Thus, measurements in the first 10–30 s, which are used to calculate the initial uptake velocity, can be done under sufficiently stable membrane-potential conditions.

All exchange velocities were calculated on the basis of kinetic measurements with at least four inhibitor-stopped exchange samples within the first 30 s. Since only the internally labeled nucleotides are measured in the exchange experiments, a formalism to calculate the initial velocity of nucleotide uptake had to be developed. This is described in the Appendix. Every point in the Eadie–Hofstee plots used for the derivation of V_{max} and K_m (cf. Figures 1 and 2) therefore includes a complete determination of an initial uptake velocity.

Results

The energy-transduction mechanism in the reconstituted adenine nucleotide transport could be elucidated on the basis of several provisions: (i) As already pointed out under Materials and Methods, defined nucleotide distributions on both sides of the membrane can be established in the reconstituted system. (ii) All exchange velocities have to be determined as initial velocities. Thus the influence of different vesicle sizes resulting in different amounts of exchanged radioactively labeled nucleotides within longer exchange times is cancelled out. (iii) It can be shown that ADP and ATP are competitive in the exchange reaction (Figure 1), though V_{max} of the nucleotide influx is dependent on the applied potential.

[1] Abbreviation: Tricine, *N*-[2-hydroxy-1,1-bis(hydroxymethyl)-ethyl]glycine.

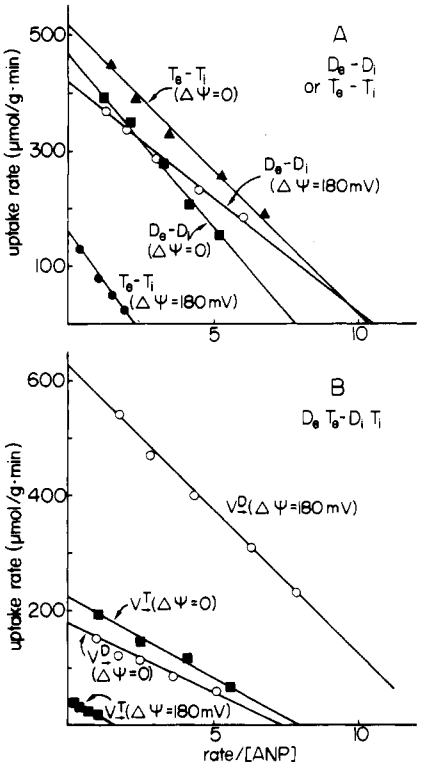

FIGURE 2: Determination of V_{max} and K_m of adenine nucleotide uptake with single homologous nucleotide distribution (A) and mixed distribution (B). Labeled external nucleotides were varied between 20 and 400 μM; internal nucleotides were 10 mM (A) or 5 mM each (B). The symbols for uptake velocity are explained in the text. Every point includes an initial velocity determination as described under Materials and Methods.

Table I: Influence of Membrane Potential and Nucleotide Distribution on the V_{max} Ratios of ADP and ATP Uptake

velocity ratio $V_{\rightarrow}^{N}$ (Δψ in mV)	nucleotide distribution[a]	
	$D_e - D_i$ and $T_e - T_i$	$D_eT_e - D_iT_i$
$V_{\rightarrow}^{D}(0)/V_{\rightarrow}^{T}(0)$	0.9 ± 0.1 (5)	0.88 ± 0.14 (3)
$V_{\rightarrow}^{D}(180)/V_{\rightarrow}^{T}(180)$	2.5 ± 0.24 (4)	10.6 ± 2.9 (7)
$V_{\rightarrow}^{D}(180)/V_{\rightarrow}^{D}(0)$	0.91 ± 0.09 (3)	3.05 ± 0.45 (4)
$V_{\rightarrow}^{T}(180)/V_{\rightarrow}^{T}(0)$	0.33 ± 0.07 (3)	0.25 ± 0.1 (4)

[a] The values are given with standard deviation and number of experiments in parentheses. Internal nucleotides were 10 mM (single) or 5 mM each (mixed).

Most of the kinetic data are obtained by a standard procedure that will be described in the following. Phospholipid vesicles with incorporated carrier protein and the appropriate nucleotide and cation distribution are used for the exchange assay. The uptake velocity is measured with external nucleotides in the range of 10–500 μM. Eadie–Hofstee plots of a typical experiment are given in Figure 2. If only one single nucleotide is present in the external space (Figure 2A), V_{max} and K_m can be directly taken from the reciprocal plot. If both ADP and ATP are present externally (Figure 2B), additional experiments have to be carried out for the calculation of K_m, where only one of the two nucleotides is varied (cf. Figure 1). It should be mentioned that the straight lines in the reciprocal plots, obtained in all experiments with reasonable accuracy, rule out a limiting influence of the internal nucleotide concentration (10 mM) on the kinetics of nucleotide uptake.

In Table I some measured uptake velocities are listed. They are given as ratios, because in different reconstituted preparations the absolute exchange activities change within about ±30% due to variable activity of the isolated and reconstituted protein and also due to variable extent of incorporation and reconstitution. The absolute velocities are furthermore strongly dependent on the type of phospholipid used for reconstitution (Krämer & Klingenberg, 1980b; Brandolin et al., 1980). All these influences can be cancelled out by calculating velocity ratios as given in Table I. Thus, the data from experiments of the same type but with different absolute uptake rates can be averaged.

In Table I the velocity ratios are given for two "basic" nucleotide distributions, namely, only one single nucleotide species with homologous distribution ($D_e - D_i$ or $T_e - T_i$) or ADP and ATP mixed in a 1:1 ratio on both sides of the membrane ($D_eT_e - D_iT_i$). The V_{max} values are found to be dependent not only on the membrane potential but also on the nucleotide distribution. The K_m values obtained in these experiments are discussed later (cf. Table V). It will be shown that, on the basis of a general kinetic model developed for the adenine nucleotide exchange, the data of Table I can be used to calculate the actual kinetic constants of ADP and ATP transport.

General Kinetic Model. The symbols used in the derivations are as follows: D, T, N, D', T', and N', concentration of ADP, ATP, or adenine nucleotides (ADP and ATP) at the outside and inside (′) of the vesicles; C_0, total carrier concentration; C, CD, CT, C', CD', and CT', concentration of free carrier, carrier–ADP, and carrier–ATP complex with binding site facing the outside and the inside (′) of the membrane; $v^D_{\rightarrow}$ and $v^T_{\rightarrow}$, ADP and ATP uptake velocities, respectively; $v^D_{\leftarrow}$ and $v^T_{\leftarrow}$, ADP and ATP efflux velocities, respectively; $V^D_{\rightarrow}$ and $V^T_{\rightarrow}$, corresponding maximum velocity; K^D_d and $K^{D'}_d$, dissociation constant of the carrier–ADP complex at the outside and inside, respectively; K^D_m and $K^{D'}_m$, concentration of ADP at the outside and inside, respectively, which yields a rate of $V/2$ for influx or efflux, named transport affinity constant; K^D and K^T, distribution constant of the carrier–ADP and carrier–ATP complexes, respectively (for derivation see text); $k^D_{\rightarrow}$, $k^D_{\leftarrow}$, $k^T_{\rightarrow}$, and $k^T_{\leftarrow}$, first-order rate constant for ADP and ATP uptake and efflux, respectively.

Some of these symbols are explained by the scheme:

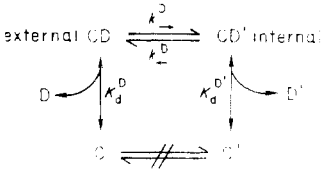

The kinetic determinations were done under two basic assumptions: (a) The overall transport rate is determined by the translocation step; i.e., the binding reaction is very fast as compared to the translocation. (b) Obligatory exchange requires that only the carrier–nucleotide complex and not the free carrier molecule is able to undergo the transition between C and C′. A corresponding conformational change has been shown to depend on the nucleotide interaction (Klingenberg, 1976).

In the following, the general rate equation for the most simple case, i.e., only ADP at the outside and inside ($D_e - D_i$), is derived. The basic equations are the mass action law equations

$$K^D_d = \frac{D \cdot C}{CD} \qquad K^{D'}_d = \frac{D' \cdot C'}{CD'} \tag{1}$$

and the conservation equation

$$C_0 = C + CD + C' + CD' \tag{2}$$

Influx and efflux are assumed to be first-order processes:

$$v^D_{\rightarrow} = k^D_{\rightarrow} CD \tag{3}$$

$$v^D_{\leftarrow} = k^D_{\leftarrow} CD' \tag{4}$$

Finally, since the ADP–ATP carrier catalyzes a strict counterexchange (Klingenberg, 1976)

$$v_{\rightarrow} = v_{\leftarrow} \tag{5}$$

Substituting eq 3 and 4 into eq 5 and after rearrangement, the following equation results:

$$CD' = CDk^D_{\rightarrow}/k^D_{\leftarrow} \tag{6}$$

This equation and eq 1 are substituted into eq 2:

$$C_0 = \frac{K^D_d}{D} CD + CD + \frac{K^{D'}_d}{D'} CD \frac{k^D_{\rightarrow}}{k^D_{\leftarrow}} + CD \frac{k^D_{\rightarrow}}{k^D_{\leftarrow}}$$

or

$$CD = \frac{DD'k^D_{\leftarrow} C_0}{K^D_d D'k^D_{\leftarrow} + (D'k^D_{\leftarrow} + K^{D'}_d k^D_{\rightarrow} + D'k^D_{\rightarrow})D} \tag{7}$$

Equation 7 can now be inserted into eq 3

$$v^D_{\rightarrow} = \frac{DD'k^D_{\leftarrow} k^D_{\rightarrow} C_0}{K^D_d k^D_{\leftarrow} D' + [K^{D'}_d k^D_{\rightarrow} + (k^D_{\leftarrow} + k^D_{\rightarrow})D']D}$$

or after rearrangement

$$v^D_{\rightarrow} = \frac{\left[\dfrac{k^D_{\rightarrow} C_0}{1 + \dfrac{k^D_{\rightarrow}}{k^D_{\leftarrow}}\left(1 + \dfrac{K^{D'}_d}{D'}\right)}\right] D}{\dfrac{K^D_d}{1 + \dfrac{k^D_{\rightarrow}}{k^D_{\leftarrow}}\left(1 + \dfrac{K^{D'}_d}{D'}\right)} + D} \tag{8}$$

It should be mentioned here that eq 8 is analogous to a classical Michaelis relation where

$$K^D_m = \frac{K^D_d}{1 + \dfrac{k^D_{\rightarrow}}{k^D_{\leftarrow}}\left(1 + \dfrac{K^{D'}_d}{D'}\right)}$$

corresponds to K_m (influx, ADP) and

$$V_{max} = \frac{k^D_{\rightarrow} C_0}{1 + \dfrac{k^D_{\rightarrow}}{k^D_{\leftarrow}}\left(1 + \dfrac{K^{D'}_d}{D'}\right)}$$

Corresponding relations can easily be derived for the nucleotide distributions $T_e - T_i$, $D_e - T_i$, or $T_e - D_i$.

The derivation of the rate equation for the situation with competition between ADP and ATP at the outside and/or inside of the vesicles is more complicated. It will be carried out only for saturating substrate concentrations ($D \gg K^D_d$ and $T \gg K^T_d$) and for a 1:1 ratio of both nucleotides ($T = D$ and $T' = D'$). The corresponding equations have to be modified into

$$C_0 = CD + CT + CD' + CT' \tag{2'}$$

$$v_{\rightarrow} = k^D_{\rightarrow} CD + k^T_{\rightarrow} CT \tag{3'}$$

$$v_{\leftarrow} = k^{D}_{\leftarrow}CD' + k^{T}_{\leftarrow}CT' \quad (4')$$

By similar insertions as above, the following equation can be derived:

$$V^{D}_{\rightarrow} = k^{D}_{\rightarrow}C_0\left[k^{D}_{\leftarrow} + k^{T}_{\leftarrow}\left(\frac{K_d^{D'}}{K_d^{T'}}\right)\right] \Big/ \left[k^{D}_{\leftarrow}\left(1 + \frac{K_d^{D}}{K_d^{T}}\right) + k^{D}_{\rightarrow}\left(1 + \frac{K_d^{D'}}{K_d^{T'}}\right) + k^{T}_{\leftarrow}\left(1 + \frac{K_d^{D}}{K_d^{T}}\right)\left(\frac{K_d^{D'}}{K_d^{T'}}\right) + k^{T}_{\rightarrow}\left(1 + \frac{K_d^{D'}}{K_d^{T'}}\right)\left(\frac{K_d^{T}}{K_d^{T'}}\right)\right] \quad (8')$$

An equivalent equation can be obtained for $v^{T}_{\rightarrow}$.

Reduced Models. The general velocity equations (eq 8 and 8′, respectively), derived above, can be reduced into two simplified models by assuming an influence of the membrane potential exclusively on the affinity of the adenine nucleotide carrier toward the bound nucleotides or on the distribution of the carrier binding site on both sides of the membrane. The two cases were elaborated originally on the nucleotide exchange in mitochondria under the influence of energization (Klingenberg, 1972). These two alternatives were also analyzed for the case of ion cotransport and termed "affinity" vs. "velocity" model (Heinz et al., 1972; Heinz & Geck, 1978; Geck & Heinz, 1976). Different from those systems, the ADP–ATP transport is a counterexchange which is basically symmetrical in the "deenergized" state of the membrane.

If the electric field regulates the adenine nucleotide exchange by changing the affinity of the carrier protein toward ADP or ATP (affinity-type model), the general velocity equation (8) for the simple nucleotide distribution $D_e - D_i$ can be modified under the following assumptions: (1) $k_{\rightarrow} = k_{\leftarrow}$, i.e., the transport rates are symmetrical; (2) $k_{\rightarrow}(\Delta\psi_1) = k_{\rightarrow}(\Delta\psi_2)$, i.e., no effect of membrane potential on the exchange rate constants. With saturating nucleotide concentrations ($D \gg K_d^{D}$), eq 8 is reduced to

$$v^{D}_{\rightarrow} = k^{D}_{\rightarrow}C_0/2 \quad (9)$$

Thus, eq 8′ gives

$$v^{D}_{\rightarrow} = k^{D}_{\rightarrow}C_0\left[k^{D}_{\leftarrow} + k^{T}_{\leftarrow}\left(\frac{K_d^{D'}}{K_d^{T'}}\right)\right] \Big/ \left[k^{D}_{\rightarrow}\left(2 + \frac{K_d^{D}}{K_d^{T}} + \frac{K_d^{D'}}{K_D^{T'}}\right) + k^{T}_{\rightarrow}\left(\frac{K_d^{D}}{K_d^{T}} + \frac{K_d^{D'}}{K_d^{T'}} + 2\left[\frac{K_d^{D}K_d^{D'}}{K_d^{T}K_d^{T'}}\right]\right)\right] \quad (9')$$

On the other hand, if the electric field influences the exchange rate constants (velocity-type model), the general rate equations can be simplified by assuming (1′) $K_d^{D} = K_d^{D'}$, i.e., the carrier affinity is symmetrical, and (2′) $K_d^{D}(\Delta\psi_1) = K_d^{D}(\Delta\psi_2)$, i.e., no effect of membrane potential on the carrier affinity. Similar as above, eq 8 and 8′ give

$$v^{D}_{\rightarrow} = k^{D}_{\rightarrow}C_0\frac{k^{D}_{\leftarrow}}{k^{D}_{\rightarrow} + k^{D}_{\leftarrow}} \quad (10)$$

and

$$v^{D}_{\rightarrow} = k^{D}_{\rightarrow}(C_0/2)\frac{k^{D}_{\leftarrow} + k^{T}_{\leftarrow}}{k^{D}_{\rightarrow} + k^{T}_{\rightarrow} + k^{D}_{\leftarrow} + k^{T}_{\leftarrow}} \quad (10')$$

For all other nucleotide distributions the corresponding rate equations, reduced to both models, have been derived by the same procedure. For methodological reasons, as discussed above, the rate values are handled in terms of the velocity ratios. The analytical expressions for these ratios as derived from the previous equations are listed in Table II, for those nucleotide distributions which are of interest in the following calculations. It will be shown that with these equations the kinetic constants can be calculated and the validity of both models tested.

Table II: Analytical Expressions for the Velocity Ratio $V^{D}_{\rightarrow}/V^{T}_{\rightarrow}$ with Different Nucleotide Distributions[a]

nucleotide distribution	velocity ratio $V^{D}_{\rightarrow}/V^{T}_{\rightarrow}$	
	affinity model	velocity model
$D_e - D_i$ and $T_e - T_i$	$\frac{k^{D}_{\rightarrow}}{k^{T}_{\rightarrow}}$	$\frac{k^{D}_{\rightarrow}}{k^{T}_{\rightarrow}}\frac{1 + K^{T}}{1 + K^{D}}$
$D_e - T_i$ and $T_e - D_i$	$\frac{k^{D}_{\rightarrow}}{k^{T}_{\rightarrow}}$	$\frac{k^{D}_{\rightarrow}}{k^{T}_{\rightarrow}}\frac{1 + k^{T}_{\rightarrow}/k^{D}_{\leftarrow}}{1 + k^{D}_{\rightarrow}/k^{T}_{\leftarrow}}$
$D_eT_e - D_iT_i$	b	$\frac{k^{D}_{\rightarrow}}{k^{T}_{\rightarrow}}$

[a] The values were derived from eq 9, 9′, 10, and 10′. Also the values for $V^{N}_{\rightarrow}(180)/V^{N}_{\rightarrow}(0)$ can be derived from these equations. [b] Very complex expression derivable from eq 9′, includes all four rate and four dissociation constants, not necessary for calculations in the text.

Calculation of Kinetic Constants. In the affinity-type model the rate constants $k_{\rightarrow}$ and the transport affinity constants K_m can be directly calculated from the reciprocal plots (cf. Figure 2) and from eq 9. In the velocity-type model the rate constants have to be derived from two different experiments, as shown below. In this calculation the value of $k^{T}_{\rightarrow}(\Delta\psi = 0)$ is used as a reference for all rate constants because the absolute values vary greatly for different phospholipid compositions of the reconstituted vesicles. As a result the value for $k^{T}_{\rightarrow}(\Delta\psi = 0) = 1$. For illustration, in extreme cases, $k_{\rightarrow}$ may vary as much as from 1 min^{-1} for phosphatidylcholine to 300 min^{-1} for phosphatidylcholine–phosphatidylethanolamine mixtures (Krämer & Klingenberg, 1980b).

For calculation of the kinetic constants in the velocity-type model, the following simplifications have to be made: (3′) For $\Delta\psi = 0$, necessarily $k^{D}_{\rightarrow} = k^{D}_{\leftarrow}$ and $k^{T}_{\rightarrow} = k^{T}_{\leftarrow}$; i.e., without membrane potential the binding site is equally distributed between both sides of the membrane. (4′) In a first approximation it is assumed that the rate constants for uptake and efflux are influenced by $\Delta\psi$ symmetrically in a reciprocal way; i.e., $k^{D}_{\rightarrow}(\Delta\psi) = f_D k^{D}_{\rightarrow}(\Delta\psi = 0)$ and $k^{D}_{\leftarrow}(\Delta\psi) = (1/f_D)k^{D}_{\leftarrow}(\Delta\psi = 0)$.

By eliminating f_D and rearrangement, the following expression can be deduced:

$$\frac{k^{D}_{\rightarrow}(\Delta\psi)}{k^{D}_{\leftarrow}(\Delta\psi)} = \frac{[k^{D}_{\rightarrow}(\Delta\psi)]^2}{k^{D}_{\rightarrow}(\Delta\psi = 0)k^{D}_{\leftarrow}(\Delta\psi = 0)}$$

and together with eq 3′

$$\frac{k^{D}_{\rightarrow}(\Delta\psi)}{k^{D}_{\leftarrow}(\Delta\psi)} = \left[\frac{k^{D}_{\rightarrow}(\Delta\psi)}{k^{D}_{\rightarrow}(\Delta\psi = 0)}\right]^2 = K^{D}(\Delta\psi) \quad (11)$$

The same is valid for ATP. With these simplifications, the distribution constants K^{D} and K^{T} can be derived from the rate constants for uptake. By inserting eq 6 into eq 11 these distribution constants can also be expressed as $K^{D} = CD'/CD$ or $K^{T} = CT'/CT$; i.e., the constants equal the ratio of carrier binding sites facing the inside to those facing the outside of the membrane.

On the basis of these relations and the experimental data of Table I, the rate constants for different nucleotide distri-

Table III: Normalized Rate Constants for Both Kinetic Models[a]

model	$k^D_{\rightarrow}$	$k^T_{\rightarrow}$	$k^D_{\leftarrow}$	$k^T_{\leftarrow}$	K^D	K^T
affinity (for all $\Delta\psi$) and velocity ($\Delta\psi = 0$)	0.9	1.0	0.9	1.0	1.0	1.0
velocity ($\Delta\psi = 180$ mV)	1.64	0.155	0.49	6.44	3.35	0.024

[a] All rate constants were normalized to $k^T_{\rightarrow} = 1.0$ (see text). The symbols are explained in the text.

butions can now be calculated. For the affinity-type model the results of the simple distributions $D_e - D_i$ and $T_e - T_i$ are sufficient to extrapolate the rate constants according to eq 9 and Table II. In the velocity-type model, since more independent constants have to be determined, the combined values for the distributions $D_e - D_i$, $T_e - T_i$, and $D_eT_e - D_iT_i$ are required. The measured velocity ratios for these nucleotide distributions (Table I) are inserted into the equations of Table II

$$\frac{k^D_{\rightarrow}}{k^T_{\rightarrow}} \frac{1 + K^T}{1 + K^D} = 2.5 \qquad (D_e - D_i,\ T_e - T_i;\ \Delta\psi = 180\ \text{mV}) \tag{12}$$

and

$$\frac{k^D_{\rightarrow}}{k^T_{\rightarrow}} = 10.6 \qquad (D_eT_e - D_iT_i;\ \Delta\psi = 180\ \text{mV}) \tag{13}$$

which can be combined to

$$K^D = 4.24K^T + 3.24 \tag{14}$$

Equation 11 is now inserted into eq 14:

$$\left[\frac{k^D_{\rightarrow}(\Delta\psi)}{k^D(\Delta\psi = 0)}\right]^2 = 4.24K^T(\Delta\psi) + 3.24 = 4.24\left[\frac{k^T_{\rightarrow}(\Delta\psi)}{k^T_{\rightarrow}(\Delta\psi = 0)}\right]^2 + 3.24 \tag{15}$$

Considering a value of 0.9 for $k^D_{\rightarrow}(\Delta\psi = 0)$ and 1.0 for $k^T_{\rightarrow}(\Delta\psi = 0)$ (cf. Table I), eq 15 reduces to

$$[k^D_{\rightarrow}(\Delta\psi)]^2/0.81 = 4.24[k^T_{\rightarrow}(\Delta\psi)]^2 + 3.24$$

Together with eq 13 one obtains the value

$$k^T_{\rightarrow}(\Delta\psi) = 0.155$$

The corresponding rate constants for ADP uptake and for nucleotide efflux can easily be calculated from eq 13, 14, and 11. These values are listed in Table III.

On the basis of the velocity-type model a definite asymmetry caused by the membrane potential can be seen. Whereas this asymmetry is not very pronounced in the case of carrier–ADP complexes, about 40 times more ATP-loaded carrier binding sites face the outside than the inside of the vesicles, due to the strongly different rate constants for influx and efflux, respectively. Although not shown in this table, also in the affinity-type model the membrane potential induces asymmetry in the adenine nucleotide transport system. This is expressed in the affinities toward ADP or ATP and will be discussed later.

Verification of the Velocity-Type Model. The aim of these calculations is now reached: all constants necessary to predict velocity ratios for other nucleotide distributions than those listed in Table I are available. The calculated velocity ratios are then compared with those measured for these distributions.

Table IV: Prediction Table of V_{max} Ratios with Nucleotide Distribution $D_e - T_i$ and $T_e - D_i$ for Both Kinetic Models

velocity ratio $V^N_{\rightarrow}(\Delta\psi$ in mV)	predicted data[a] affinity model	predicted data[a] velocity model	measured data[b]
$V^D_{\rightarrow}(0)/V^T_{\rightarrow}(0)$	0.9	1.0	0.9 ± 0.12
$V^D_{\rightarrow}(180)/V^T_{\rightarrow}(180)$	0.9	11.1	8.3 ± 2.3
$V^D_{\rightarrow}(180)/V^D_{\rightarrow}(0)$	1.0	2.75	2.55 ± 0.3
$V^T_{\rightarrow}(180)/V^T_{\rightarrow}(0)$	1.0	0.25	0.28 ± 0.08

[a] The predicted data are calculated from exchange experiments with the distributions $D_e - D_i$, $T_e - T_i$, and $D_eT_e - D_iT_i$ (see text). [b] The measured values are given for the distributions $D_e - T_i$ and $T_e - D_i$.

Table V: K_m Values (μM) for ADP and ATP Uptake with Different Nucleotide Distributions[a]

nucleotide distribution	$\Delta\psi = 0$ ADP	$\Delta\psi = 0$ ATP	$\Delta\psi = 180$ mV ADP	$\Delta\psi = 180$ mV ATP
$D_e - D_i$ and $T_e - T_i$	60 ± 6 (4)	56 ± 11 (4)	30 ± 6 (4)	95 ± 10 (3)
$D_e - T_i$ and $T_e - D_i$	65 ± 13 (4)	52 ± 16 (4)	75 ± 21 (3)	68 ± 18 (3)
$D_eT_e - D_iT_i$	56 ± 5 (3)	52 ± 15 (3)	36 ± 9 (7)	325 ± 65 (7)

[a] The data are derived from experiments as shown in Figures 1 and 2. They are given with standard deviation and number of experiments in parentheses.

By this, both models can be tested for their validity. In Table IV the comparison is carried out for the distributions $D_e - T_i$ and $T_e - D_i$, i.e., single nucleotides on both sides but heterologous distribution. The predicted velocity ratios are calculated by inserting the rate constants of Table III into the equations of Table II. The values in Table IV for the affinity-type model seem to be trivial. However, that is due to this particular case of single heterologous nucleotide distribution, which gives such trivial ratios of the V_{max} values.

From these results it is obvious that only the ratios predicted by the velocity-type model agree with the measured data. Also, to other types of mixed nucleotide distributions (e.g., mixed inside and single outside, or vice versa) this procedure can be applied, yielding basically similar results. However, the results are more conclusive in the case of the extreme single heterologous distribution of Table IV which can be achieved only in a reconstituted system.

Substrate Affinity. So far, the discrimination between the two models on the basis of calculated rate constants is convincing. But how can we explain the observed changes in the carrier–substrate affinity? The transport affinity constants K_m derived from experiments as shown in Figures 1 and 2 are given for several nucleotide distributions in Table V. It is evident that the K_m values for the adenine nucleotide uptake are definitely affected not only by $\Delta\psi$ but also by the type of nucleotide distribution under which they have been measured. However, the dissociation constants K_d, of which K_m is a function according to eq 8, do not change whether a homologous or heterologous nucleotide distribution is applied. The substrate affinity should only be an attribute of the carrier protein conformation and should not reflect the nucleotide distribution over the membrane.

Also the true K_d values can be calculated by inserting the data from Table V into eq 8 under the experimental conditions of internally saturating nucleotide concentrations ($N' \gg K_d'$). These values cannot be used for discrimination of the models because they cannot directly be measured. However, similar

Table VI: Prediction Table of K_m Values (μM) with Nucleotide Distributions $D_e - T_i$ and $T_e - D_i$ and $\Delta\psi$ = 180 mV for Both Kinetic Models

	predicted data[a]		
	affinity model	velocity model	measured data[b]
K_m^D	30	95	75 ± 21 (3)
K_m^T	95	81	68 ± 18 (3)

[a] The predicted data are calculated from exchange experiments with the distributions $D_e - D_i$ and $T_e - T_i$ (see text). [b] The measured values are given for the distributions $D_e - T_i$ and $T_e - D_i$.

to the procedure carried out with the rate constants, these dissociation constants, calculated for the nucleotide distributions $D_e - D_i$ and $T_e - T_i$, can be used to predict K_m values for the heterologous distributions $T_e - D_i$ and $D_e - T_i$. This is shown in Table VI.

Although the K_m values do not allow a discrimination between the two models as clear as the rate constants, it is nevertheless obvious that the values predicted by the velocity-type model resemble much closer the experimental data. In conclusion, also on the basis of the observed substrate affinity of the adenine nucleotide carrier, the velocity-type model shows significantly better agreement with the measured data than the affinity-type model. It has to be pointed out once more that the measured K_m values, especially with mixed nucleotide distribution (cf. line 3 in Table V), do actually change under the influence of membrane potential. However, these changes, as derived above, reflect a strong influence of the potential on the rate constants $k_{\rightarrow}$ and $k_{\leftarrow}$ and not on the dissociation constants K_d, both of which are implicated in the transport affinity constants K_m.

Discussion

The transport of adenine nucleotides across the inner mitochondrial membrane is modulated by the membrane potential (LaNoue et al., 1978; Klingenberg & Rottenberg, 1977; Krämer & Klingenberg, 1980a). The mechanism of this regulation, however, is still controversially explained. A detailed examination of this problem is possible with the reconstituted carrier protein, based on several advantages of this system: (i) widely varying and well-defined nucleotide distributions between the internal and external spaces can be established; (ii) the ATP/ADP ratios are not disturbed by ATPase or adenylate kinase (Krämer & Klingenberg, 1980a); (iii) these ratios do not have to be corrected for the complexation effects of Mg^{2+}, the free concentration of which in the matrix space of mitochondria is not exactly known (Krämer, 1980).

With these favorable experimental conditions it seemed promising to describe the adenine nucleotide exchange by a general equation, which allows differentiation between a regulatory influence of the "energization" on the K_d or on the rate constants $k_{\rightarrow}$. This equation, however, turned out to be too complex for an experimental verification, and thus reduced models restricting the influence of membrane potential either on the binding affinity (affinity-type model) or on the distribution of the binding site (velocity-type model) were introduced. In the reconstituted system the conditions (concentration and ADP–ATP distribution) could be chosen such that the equation is further simplified and thus became amenable to the experimental test.

On the basis of the data presented here and furthermore supported by experiments in earlier reports, a decision between both models for the carrier regulation is possible.

(1) The kinetic equations described above offer the possibility to predict velocity ratios according to both theoretically possible models if particular nucleotide distributions are chosen. As shown in Table IV, only the data predicted by the velocity-type model agree with the measured data. A striking asymmetry of the distribution of carrier binding sites under the influence of membrane potential can be seen (Table III).

(2) The same, although not as conclusive as for the rate constants, holds true for the transport affinity constants K_m (Table VI). It should be emphasized here again that also in the velocity-type model K_m may change without a simultaneous change in the K_d. In other words, the clear alteration of K_m (5–10 times, Table V) is not necessarily supporting the affinity model.

(3) It should be taken into account that the affinity-type model implies a conformational change of the carrier protein directly caused by the membrane potential. However, it seems to be rather improbable that this change in the binding affinity with respect to protein conformation is correlated to membrane potential with infinitely small steps. A linear relation between the uptake velocity ratio of ATP/ADP and $\Delta\psi$ has been shown earlier (Krämer & Klingenberg, 1980a). Even more inexplicable is the fact that the exchange regulation is effective in the reciprocal manner when the membrane potential is reversed to the opposite direction, i.e., negatively charged outside (Krämer & Klingenberg, 1980a). In the affinity-type model, this should be due to a reciprocal conformation change of the carrier protein, which, however, would never occur in its physiological function. On the other hand, this phenomenon is easily explained in the velocity-type model by simply modulating the rate constants, which are influenced electrophoretically by the membrane potential.

(4) The only arguments so far supporting the affinity-type model for the regulation of the adenine nucleotide transport in mitochondria are the experiments of Souverijn et al. (1973), Vignais et al. (1975), Villiers et al. (1979), and Lauquin et al. (1978). However, in our hands, in detailed kinetic experiments with mitochondria the large affinity changes have never been seen (Klingenberg, 1972; Weidemann et al., 1970). The values measured by Souverijn et al. (1973) are transport affinities K_m which have been shown here to include the dissociation constants in a complex relation. In other words, changes of the measured K_m do not mean also changes of K_d to the same extent. Nevertheless, the reported 100-fold increase for K_m^T is too large to be explained by the velocity model. However, there are experimental reasons for the conclusion that the changes reported by Souverijn et al. (1973) are much too large. At any rate, the K_m values determined in our laboratory, first by manual stopping (Pfaff et al., 1969) and later by automated quench sampling (Klingenberg, 1976), increase only slightly on energization, K_m^T by 2.5-fold and K_m^D by 1.5-fold.

There are also other reasons to assume that the results obtained in the reconstituted system are valid also for the carrier protein in its physiological surroundings. In earlier reports it has been shown that the reconstituted adenine nucleotide carrier has the same properties as in mitochondria in respect to inhibitor binding (Krämer & Klingenberg, 1977a), specific exchange activity (Krämer & Klingenberg, 1977b, 1979), and regulation by membrane potential (Krämer & Klingenberg, 1980a). It is highly improbable therefore that the reconstituted carrier protein, though resembling the mitochondrial functions in all these properties, should completely change its mechanism of exchange regulation from the affinity

type to the velocity type when brought from the inner mitochondrial membrane to an artificial phospholipid vesicle.

In another respect, however, the incorporated carrier protein does seem to be different from the physiological situation. The measured transport affinity K_m is about 5–10 times higher when the carrier is incorporated into liposomes. This discrepancy can be largely reduced if other phospholipid compositions, more similar to the inner mitochondrial membrane, are used for the reconstituted vesicles. With freshly prepared phosphatidylcholine and phosphatidylethanolamine from egg yolk in a 1:1 ratio, for example, values for K_m of about 9–12 μM can be measured (experiments not shown) which are very close to the physiological values of 3–10 μM (Weidemann et al., 1970; Pfaff et al., 1969).

The conclusion, that the velocity-type model is valid for the regulation of the ADP–ATP carrier, has important consequences for an interpretation of the energy transduction mechanism. No conformation change, directly induced by the membrane potential, is involved. The basic principle proves to be an electrophoretic process exerting influence primarily on the carrier–ATP complex in which the binding center with bound ATP is visualized to carry one extra negative charge. Thus, it leads to an extremely asymmetric distribution of the ATP binding site on both sides of the membrane (cf. Table III).

It has to be taken into account, however, that the carrier protein exists in two conformations, i.e., c conformation when the binding site is exposed to the cytosol and m conformation when it faces the matrix (Klingenberg, 1976; Klingenberg & Appel, 1980). In the transport reaction, the carrier alternates between these two conformations, according to the well-described mechanism. Since the membrane potential shifts the distribution of binding sites between inside and outside, it also influences the distribution of carrier molecules between the m and the c state, respectively. Thus, the membrane potential indirectly influences the c and m conformational transition, although this is not comparable with a direct potential-induced electrostriction effect on the protein as it would be required in the affinity-type model.

Acknowledgments

We thank G. Kürzinger and S. Tsompanidou for skillful technical assistance and A. Munding for his assistance in the derivation of the initial uptake velocity.

Appendix

Derivation of Initial Uptake Velocity. The symbols are the same as used above; $^*N$ means radioactive label belonging to nucleotides (dpm) and $^*v_{\rightarrow}$ or $^*v_{\leftarrow}$ means uptake or efflux velocity of radioactive label (dpm) into or out of the vesicles, which can be expressed as

$$^*v_{\rightarrow} = v_{\rightarrow}{}^*N/N \quad \text{(A1)}$$

$$^*v_{\leftarrow} = v_{\leftarrow}{}^*N'/N' \quad \text{(A2)}$$

Together with the basic exchange equation (5) the increase of radioactive label internally, which is the actual value to be measured in the experiments, can be obtained

$$\frac{\mathrm{d}^*N'}{\mathrm{d}t} = {}^*v_{\rightarrow} - {}^*v_{\leftarrow} = v\left(\frac{^*N}{N} - \frac{^*N'}{N'}\right) = v\left(\frac{^*N_0 - {}^*N'}{N} - \frac{^*N}{N'}\right) = -\frac{N + N'}{NN'}v{}^*N' + \frac{^*N_0}{N'}v \quad \text{(A3)}$$

where $^*N_0$ = sum of externally added label at the beginning of the experiment and v = uptake velocity. Setting $k = [(N + N')/(NN')]v$ we obtain

$$\frac{\mathrm{d}^*N'}{\mathrm{d}t} = -k{}^*N' + \frac{^*N_0}{N}v \quad \text{(A4)}$$

Equation A4 is integrated and leads to

$$^*N' = e^{-kt}\left[\int \frac{^*N_0}{N}ve^{kt}\,\mathrm{d}t + C\right] = e^{-kt}\left[\frac{^*N_0}{N}\frac{v}{k}e^{kt} + C\right]$$

which can be rewritten as

$$^*N' = \frac{^*N_0N'}{N + N'} + Ce^{-kt} \quad \text{(A5)}$$

If $t = 0$ (start conditions) and $^*N' = 0$, which is inserted into eq A5

$$C = -\frac{^*N_0N'}{N + N'}$$

Together with eq A5 we obtain

$$^*N' = \frac{^*N_0N'}{N + N'}(1 - e^{-kt})$$

which can now be inserted into eq A3:

$$^*v_{\rightarrow} - {}^*v_{\leftarrow} = \frac{\mathrm{d}^*N'}{\mathrm{d}t} = \frac{^*N_0}{N}ve^{-kt}$$

or

$$\ln\,(^*v_{\rightarrow} - {}^*v_{\leftarrow}) = -\frac{N + N'}{NN'}vt + \ln\frac{^*N_0}{N}v \quad \text{(A6)}$$

$\ln\,(^*v_{\rightarrow} - {}^*v_{\leftarrow})$, which represents the measured increase in internal radioactive label, is plotted against exchange time t. The extrapolated segment on the velocity axis equals $\ln\,(^*N_0/N)v$. Thus, v, the initial uptake velocity, can be calculated.

References

Booth, I. R., & Hamilton, W. A. (1980) *Biochem. J. 188*, 467–473.

Brandolin, G., Doussiere, J., Gulik, A., Gulik-Krzywicki, T., Lauquin, G. J. M., & Vignais, P. V. (1980) *Biochim. Biophys. Acta 592*, 592–614.

Chen, D. S., Jr., Toribara, T. Y., & Warner, H. (1956) *Anal. Chem. 28*, 1756.

Geck, P. (1971) *Biochim. Biophys. Acta 241*, 462–472.

Geck, P., & Heinz, E. (1976) *Biochim. Biophys. Acta 443*, 49–63.

Heinz, E., & Geck, P. (1978) *Membr. Transp. Processes 1*, 13–30.

Heinz, E., Geck, P., & Willbrandt, W. (1972) *Biochim. Biophys. Acta 255*, 442–461.

Helenius, A., & Simons, K. (1972) *J. Biol. Chem. 247*, 3656–3661.

Holman, G. D. (1980) *Biochim. Biophys. Acta 599*, 202–213.

Kaczorowski, G. J., Robertson, D. E., & Kaback, R. E. (1979) *Biochemistry 18*, 3697–3704.

Kasahara, M., & Hinkle, P. C. (1977) *J. Biol. Chem. 252*, 7384–7390.

Klingenberg, M. (1972) *Mitochondria: Biomembranes*, pp 147–162, Elsevier, Amsterdam.

Klingenberg, M. (1975) *Energy Transform. Biol. Systems, Ciba Found. Symp., 1975 No. 31*, 23–68.

Klingenberg, M. (1976) in *The Enzymes of Biological Membranes: Membrane Transport* (Martonosi, A. N., Ed.) Vol. 3, pp 383–438, Plenum Press, New York and London.

Klingenberg, M. (1980) *J. Membr. Biol. 56*, 97–105.
Klingenberg, M., & Pfaff, E. (1966) in *Regulation of Metabolic Processes in Mitochondria* (Tager, J. M., et al., Eds.) pp 180–201, Elsevier, Amsterdam.
Klingenberg, M., & Rottenberg, H. (1977) *Eur. J. Biochem. 73*, 125–130.
Klingenberg, M., & Appel, M. (1980) *FEBS Lett. 119*, 195–199.
Klingenberg, M., Wulf, R., Heldt, H. W., & Pfaff, E. (1969) in *Mitochondria: Structure and Function* (Ernster, L., & Drahota, Z., Eds.) pp 59–77, Academic Press, London and New York.
Komor, E., Haass, D., Komor, B., & Tanner, W. (1973) *Eur. J. Biochem. 39*, 193–200.
Krämer, R. (1980) *Biochim. Biophys. Acta 592*, 615–620.
Krämer, R., & Klingenberg, M. (1977a) *Biochemistry 16*, 4954–4961.
Krämer, R., & Klingenberg, M. (1977b) *FEBS Lett. 82*, 363–367.
Krämer, R., & Klingenberg, M. (1979) *Biochemistry 18*, 4209–4215.
Krämer, R., & Klingenberg, M. (1980a) *Biochemistry 19*, 556–560.
Krämer, R., & Klingenberg, M. (1980b) *FEBS Lett. 119*, 257–260.
Krämer, R., Aquila, H., & Klingenberg, M. (1977) *Biochemistry 16*, 4949–4953.
Lancaster, J. R., Jr., Hill, R. J., & Struve, W. G. (1975) *Biochim. Biophys. Acta 401*, 285–298.
LaNoue, K., Mizani, S. M., & Klingenberg, M. (1978) *J. Biol. Chem.* 253, 191–198.
LaNoue, K., Duszynski, J., Watts, J. A., & McKee, E. (1979) *Arch. Biochem. Biophys. 195*, 578–590.
Lauquin, G. J. M., Villiers, C., Michejda, J., Brandolin, G., Boulay, F., Cesarini, R., & Vignais, P. V. (1978) in *The Proton and Calcium Pumps* (Azzone, G. F., et al., Eds.) pp 251–262, Elsevier and North Holland, Amsterdam.
Murphy, E., Coll, K. E., Viale, R. O., Tischler, M. E., & Williamson, J. R. (1979) *J. Biol. Chem. 254*, 8369–8376.
Pfaff, E., Heldt, H. W., & Klingenberg, M. (1969) *Eur. J. Biochem. 10*, 484–493.
Schwab, W. G. W., & Komor, E. (1978) *FEBS Lett. 87*, 157–160.
Souverijn, J. H. M., Huisman, L. A., Rosing, J., & Kemp, A., Jr. (1973) *Biochim. Biophys. Acta 305*, 185–198.
Vignais, P. V., Vignais, P. M., & Doussiere, J. (1975) *Biochim. Biophys. Acta 376*, 219–230.
Villiers, C., Michejda, J. W., Block, M., Lauquin, G. J. M., & Vignais, P. V. (1979) *Biochim. Biophys. Acta 546*, 157–170.
Weidemann, M. J., Erdelt, H., & Klingenberg, M. (1970) *Eur. J. Biochem. 16*, 313–335.
Wright, J. K., Teather, R. M., & Overath, P. (1979) in *Function and Molecular Aspects of Biomembrane Transport* (Quagliariello, E., et al., Eds.) pp 239–248, Elsevier and North Holland, Amsterdam.